Elliptic Lagrangian Coherent Structures in geophysical fluid flows

F. J. Beron-Vera

Rosenstiel School of Marine and Atmospheric Science
University of Miami

Collaborators: M. Olascoaga, M. Brown and H. Koçack

Vienna, 8 May 2012.

fberon@rsmas.miami.edu
www.math.miami.edu/fberon

Acknowledgements

Research supported by U.S. NSF, NASA and NIEHS.

Hyperbolic LCS: transport and mixing

20-Apr-2010

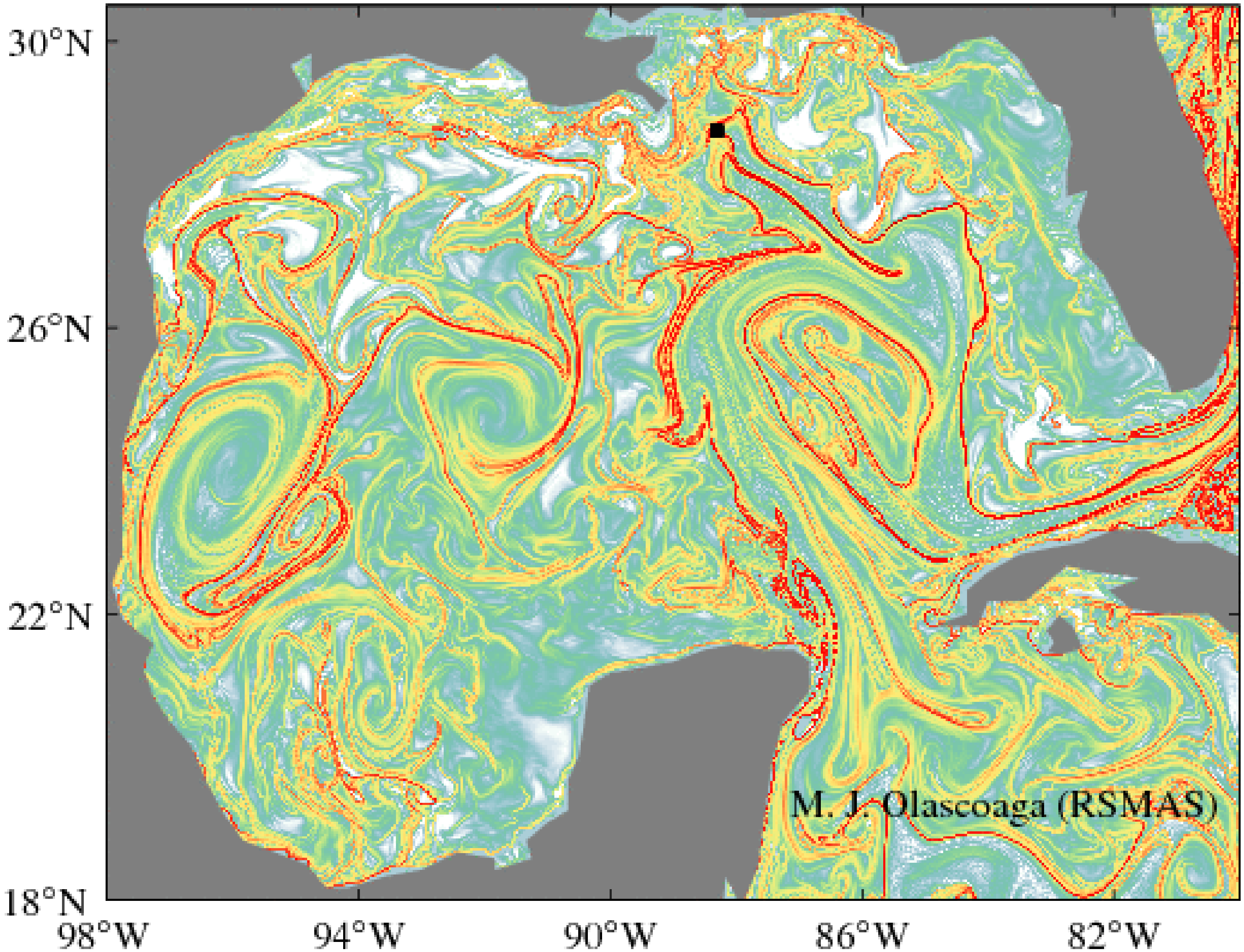

Physica D 240 (2011) 574–598

Contents lists available at ScienceDirect

Physica D

journal homepage: www.elsevier.com/locate/physd

A variational theory of hyperbolic Lagrangian Coherent Structures

George Haller *

Department of Mechanical Engineering, McGill University, 817 Sherbrooke Ave. West, Montreal, Quebec H3A 2K6, Canada
Department of Mathematics and Statistics, McGill University, 817 Sherbrooke Ave. West, Montreal, Quebec H3A 2K6, Canada

ARTICLE INFO

Article history:
Received 6 July 2010
Received in revised form
12 November 2010
Accepted 17 November 2010
Available online 10 December 2010
Communicated by V. Rom-Kedar

Keywords:
Lagrangian Coherent Structures
Invariant manifolds
Mixing

ABSTRACT

We develop a mathematical theory that clarifies the relationship between observable Lagrangian Coherent Structures (LCSs) and invariants of the Cauchy–Green strain tensor field. Motivated by physical observations of trajectory patterns, we define hyperbolic LCSs as material surfaces (i.e., codimension-one invariant manifolds in the extended phase space) that extremize an appropriate finite-time normal repulsion or attraction measure over all nearby material surfaces. We also define weak LCSs (WLCSs) as stationary solutions of the above variational problem. Solving these variational problems, we obtain computable sufficient and necessary criteria for WLCSs and LCSs that link them rigorously to the Cauchy–Green strain tensor field. We also prove a condition for the robustness of an LCS under perturbations such as numerical errors or data imperfection. On several examples, we show how these results resolve earlier inconsistencies in the theory of LCS. Finally, we introduce the notion of a Constrained LCS (CLCS) that extremizes normal repulsion or attraction under constraints. This construct allows for the extraction of a unique observed LCS from linear systems, and for the identification of the most influential weak unstable manifold of an unstable node.

Elliptic LCS: transport barrier

The Antarctic “ozone hole”

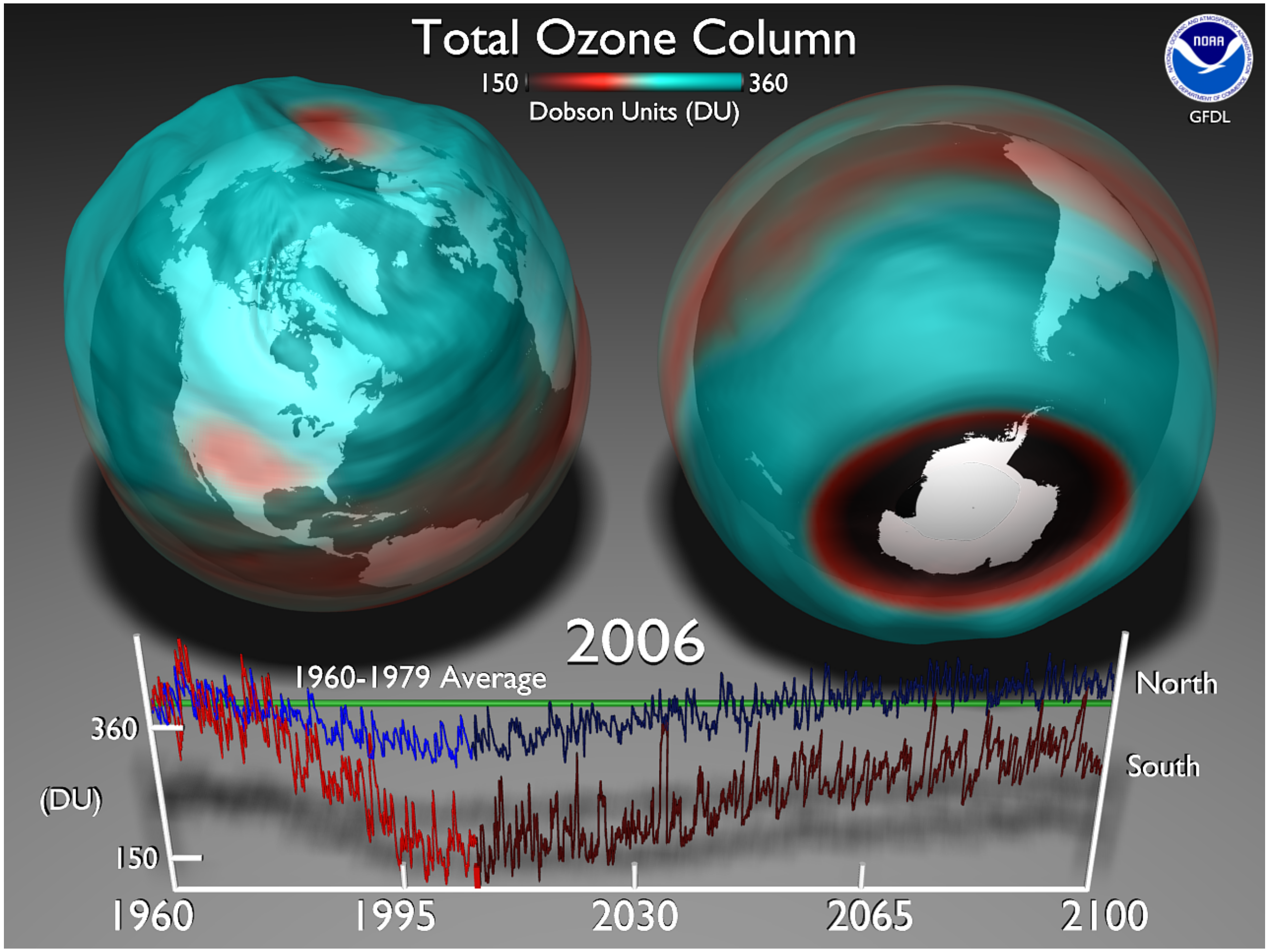

Cold air confined within the stratospheric polar vortex and sunlight facilitate the chemical reactions leading to natural ozone depletion; best conditions achieved in the Austral springtime; stimulated by CFC production, which was limited by the Montreal Protocol.

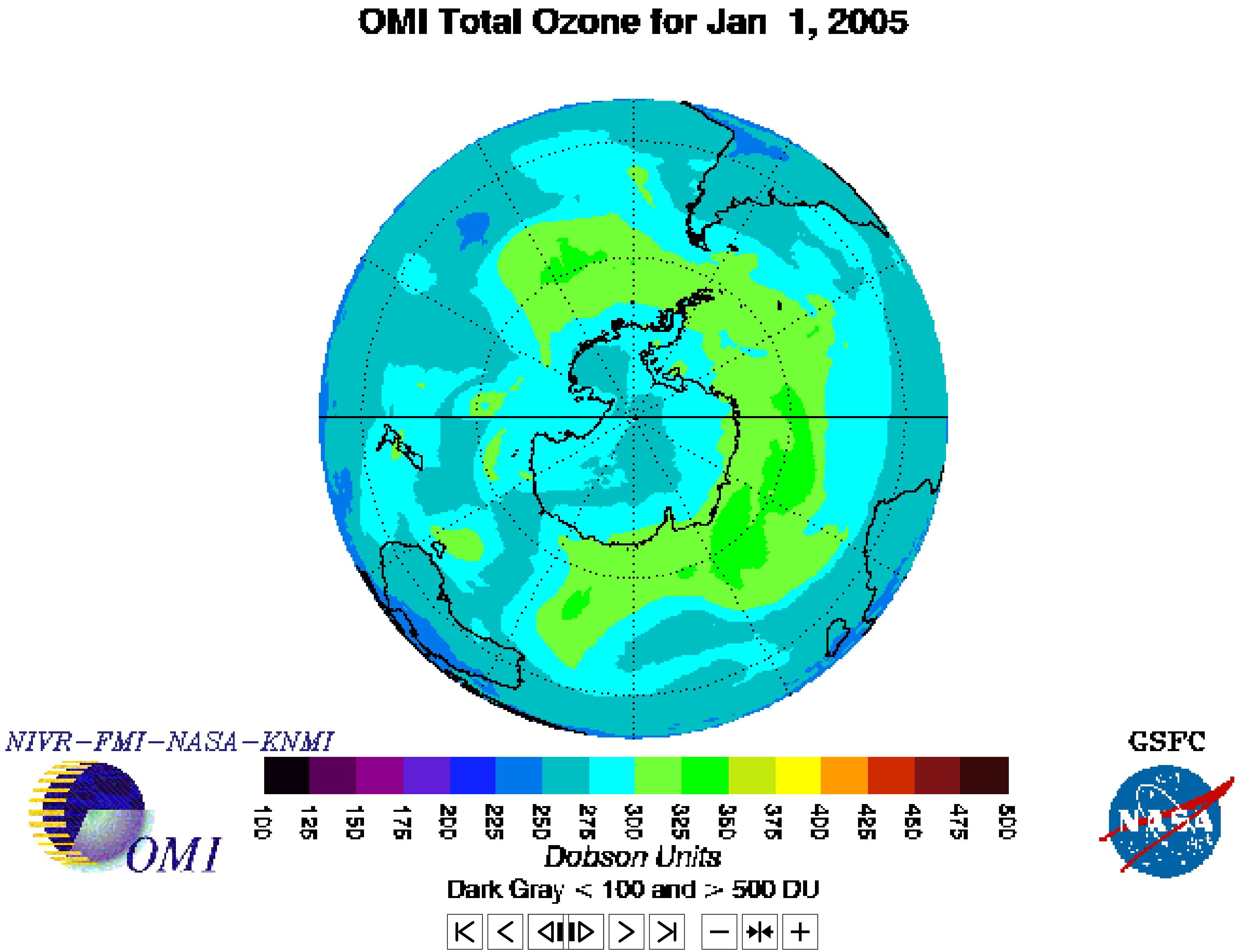

OMI Total Ozone for Jan 1, 2005
NIVR−FMI−NASA−KNMI
OMI
100 125 150 175 200 225 250 275 300 325 350 375 400 425 450 475 500
Dobson Units
Dark Gray < 100 and > 500 DU
GSFC
NASA

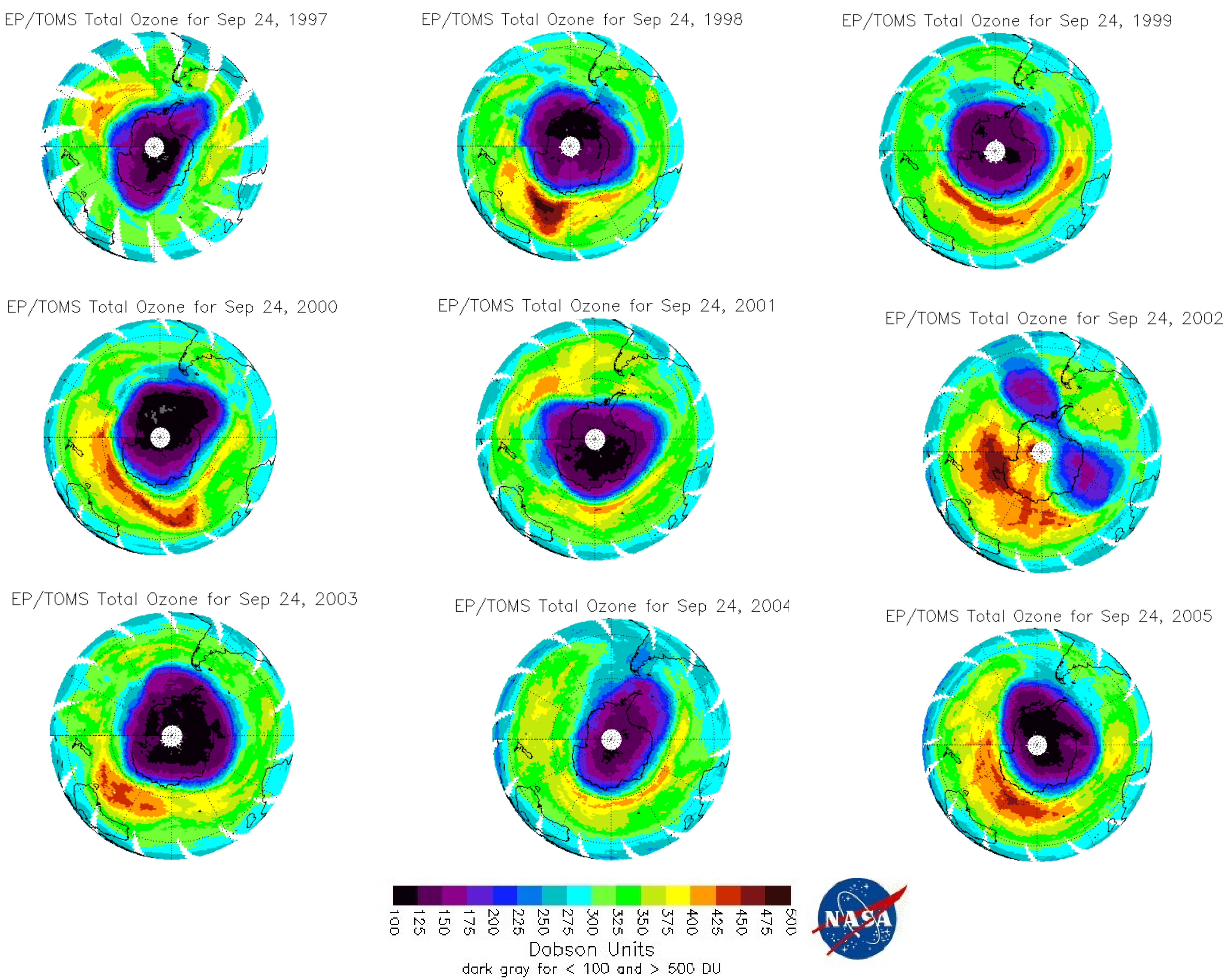
EP/TOMS Total Ozone for Sep 24, 1997
EP/TOMS Total Ozone for Sep 24, 1998
EP/TOMS Total Ozone for Sep 24, 1999
EP/TOMS Total Ozone for Sep 24, 2000
EP/TOMS Total Ozone for Sep 24, 2001
EP/TOMS Total Ozone for Sep 24, 2002
EP/TOMS Total Ozone for Sep 24, 2003
EP/TOMS Total Ozone for Sep 24, 2004
EP/TOMS Total Ozone for Sep 24, 2005
100 125 150 175 200 225 250 275 300 325 350 375 400 425 450 475 500
Dobson Units
dark gray for < 100 and > 500 DU

Mount Pinatubo's sulfur dioxide and dust aerosol plume

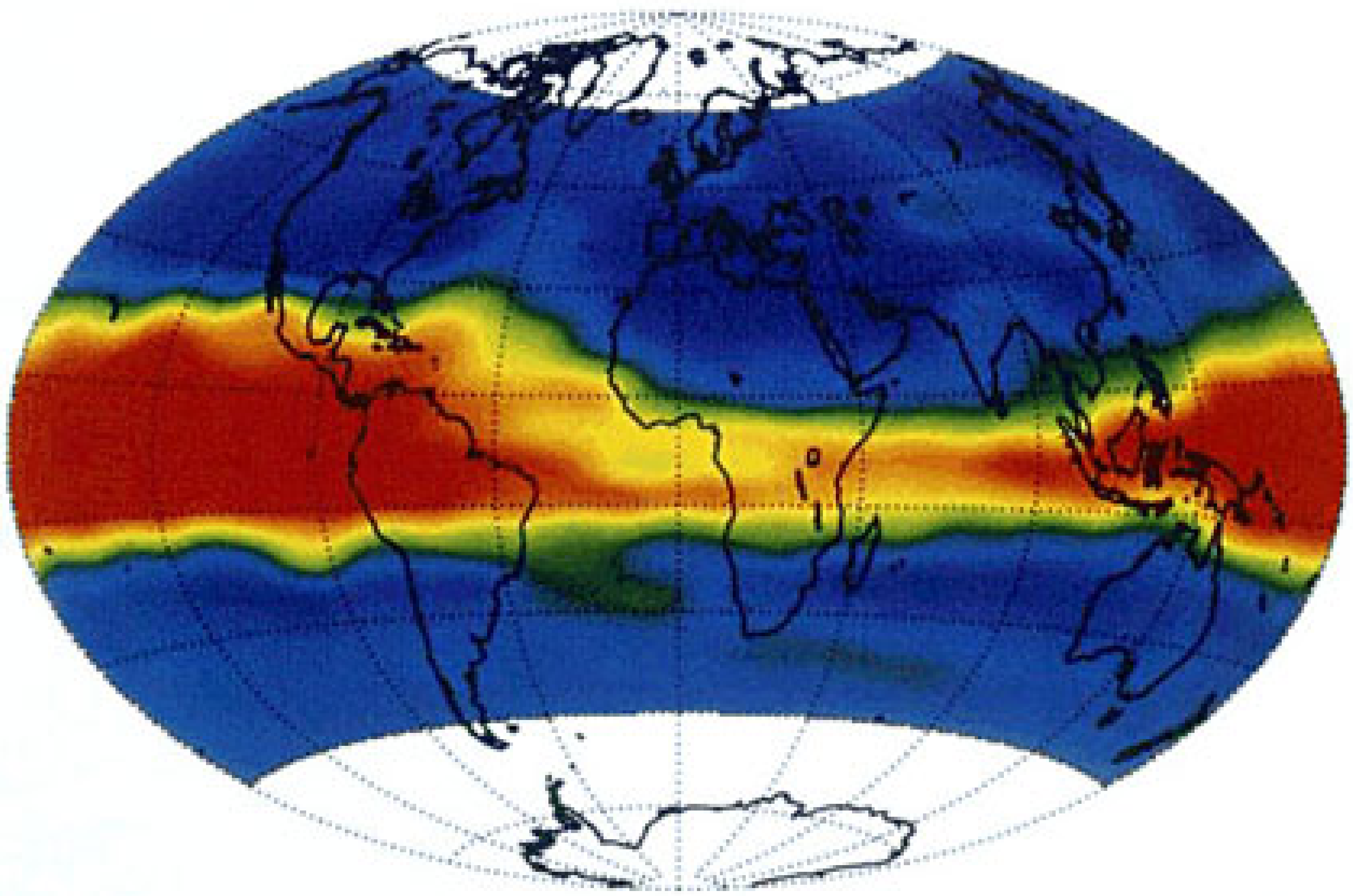

Approximately 45 days after the eruption on 12 June 1991, the aerosol plume completely circled the Earth around the equator forming a band 20 to 50° of latitude wide.

Jupiter's belts and zones

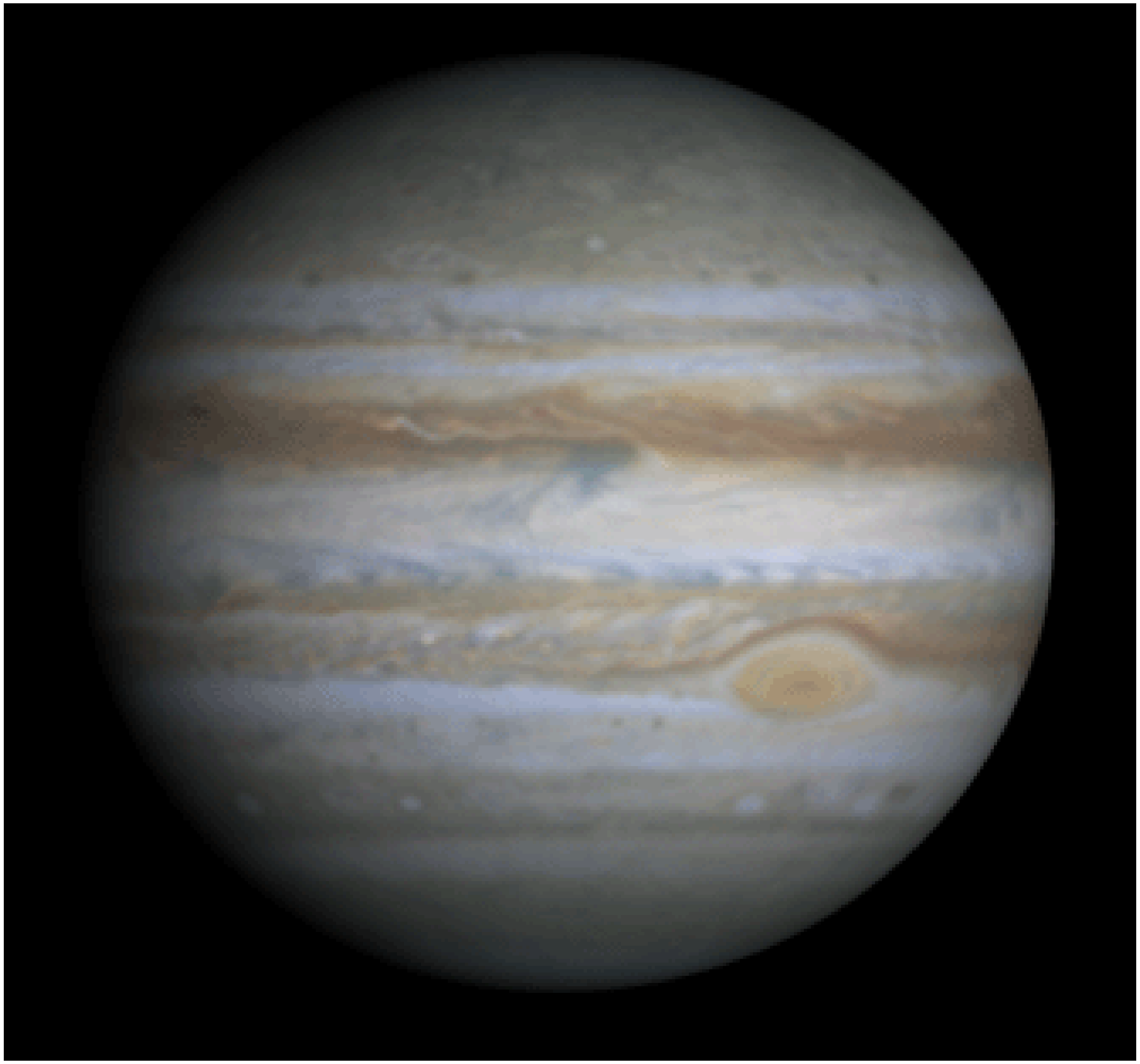

Belts (bright bands) and zones (dark bands) differ in chemical composition.

Sea surface temperature fronts in the ocean

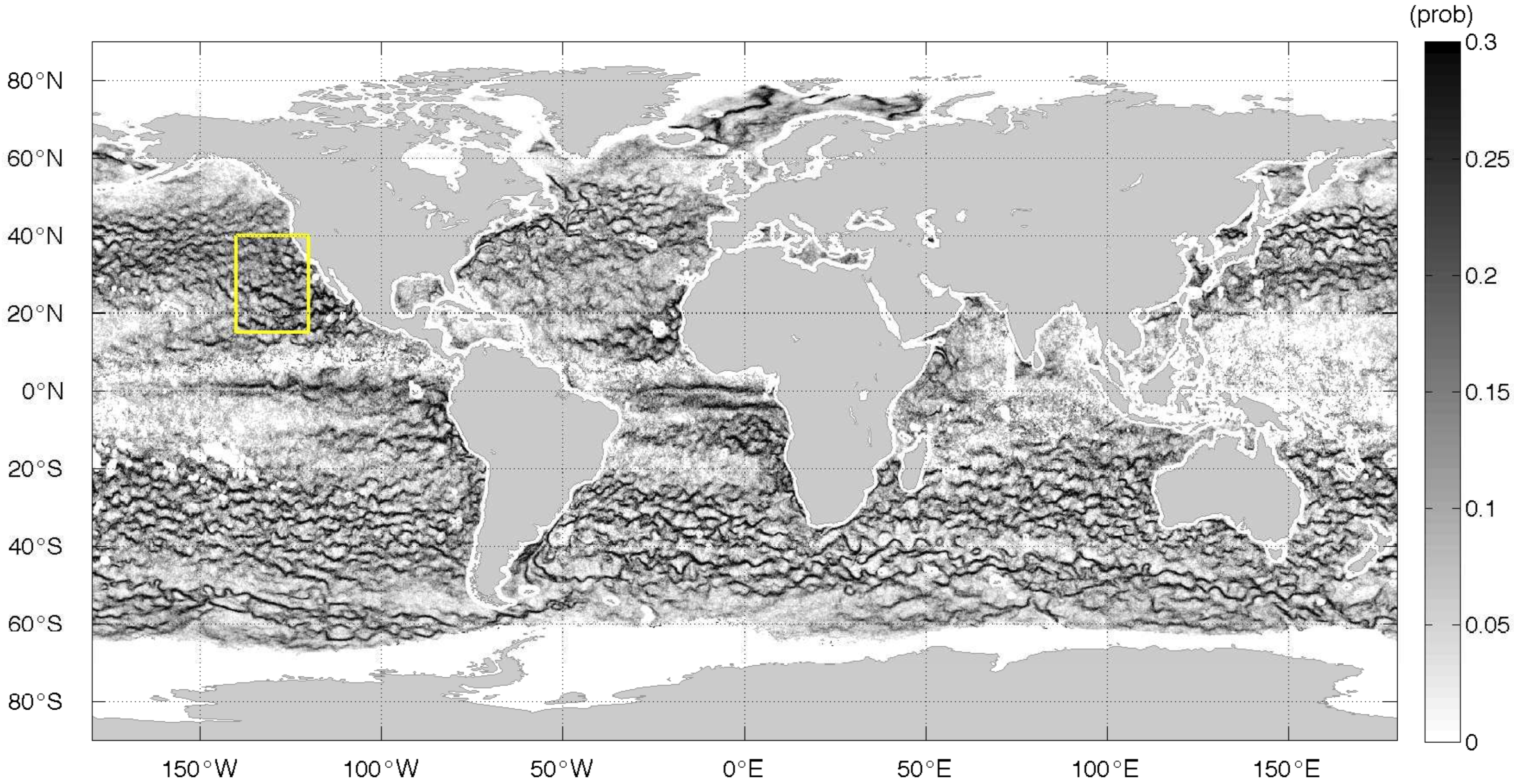

Courtesy C. Buckingham.

Zonal jets as transport barriers

Seasonal variation of stratospheric zonally-averaged zonal wind and potential vorticity from CMAM model

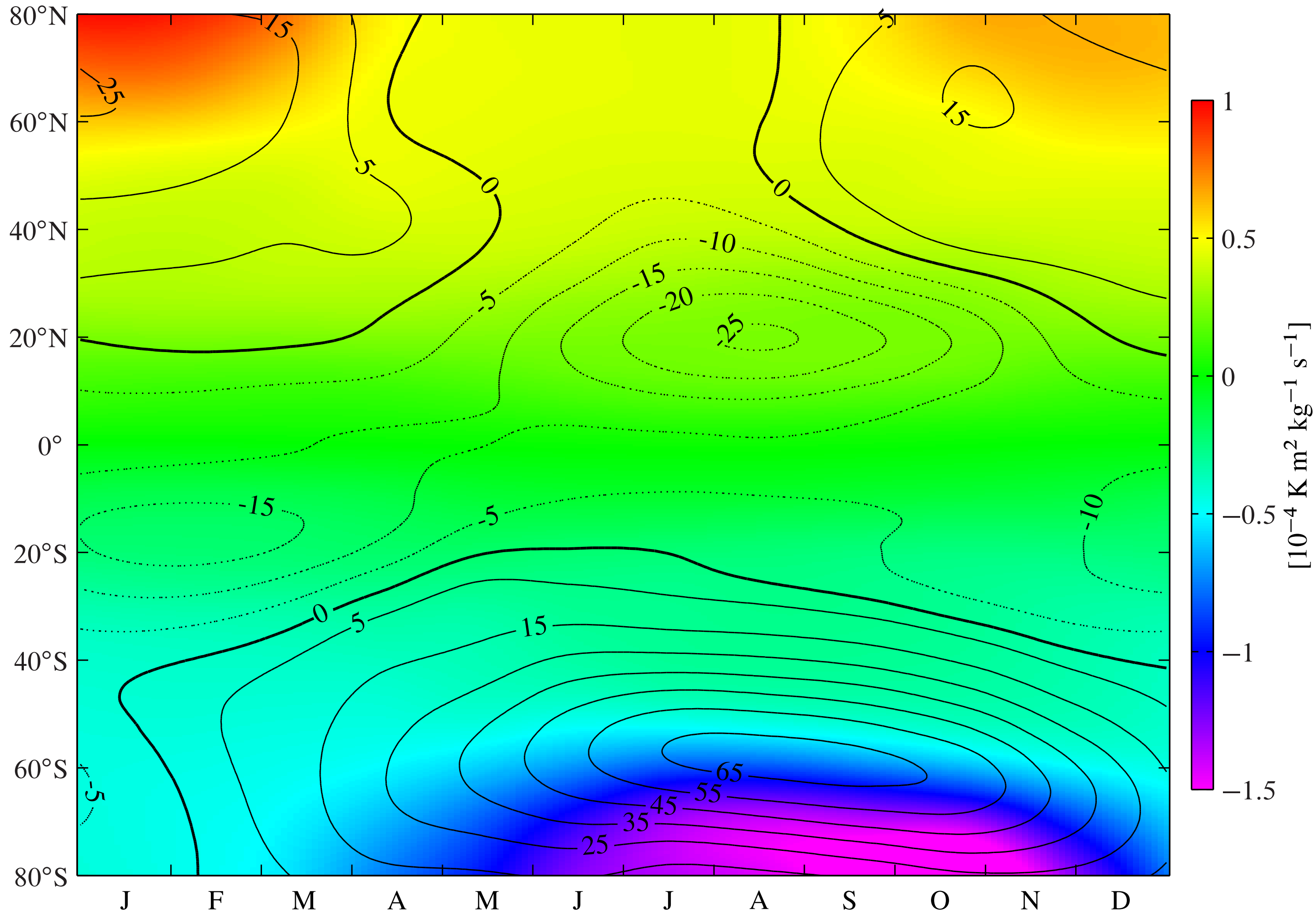

The Potential Vorticity (PV) is a measure of swirl (including the planetary rotation) which is transported by the fluid.

Jupiter’s top-cloud level winds

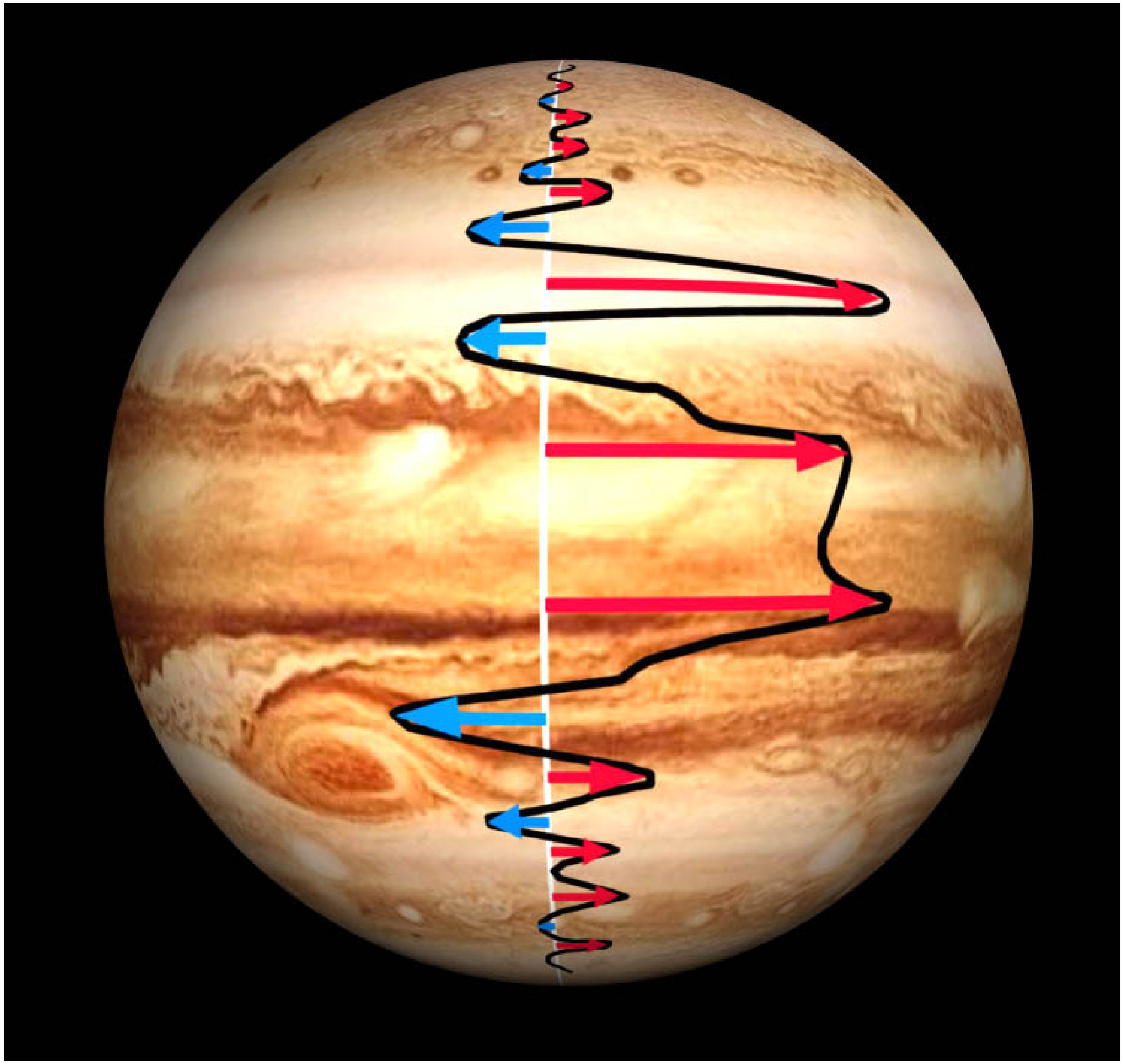

Axes of alternating eastward and westward jets coincide with boundaries between belts and zone.

Zonal jets in the ocean

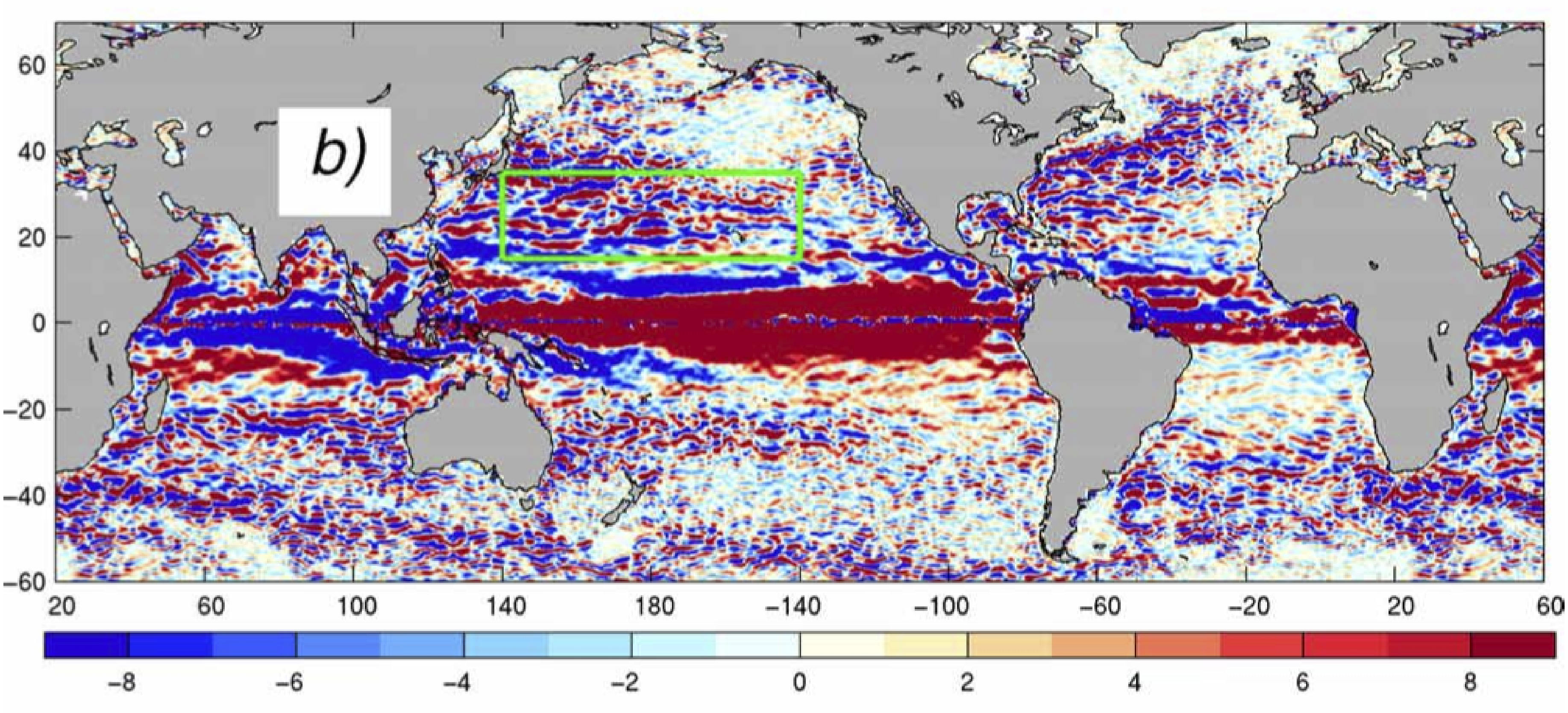

From Maximenko et al. (2006).

The reminder of the talk

- Setup; KAM theorem; "strong KAM stability" [Rypina et al., 2007a,b; FJBV et al., 2010].
- The Bickley jet; kinematic model of zonal eastward jet perturbed with Rossby waves [del-Castillo-Negrete and Morrison, 1993; Rypina et al., 2007b; FJBV et al., 2010].
- The stratospheric austral polar night jet; eastward jet at the edge of the stratospheric polar vortex in the austral winter/spring; strong PV gradient associated; realistic simulation based on the Canadian Middle-Atmosphere Model (CMAM) [FJBV et al., 2010, 2011].
- The stratospheric boreal summer subtropical jet; *westward* jet that develops in the subtropics during the boreal summer/fall; *weak* PV gradient associated; also based on CMAM [FJBV et al., 2011].
- Jovian jets; dynamically consistent nonlinear evolution of perturbed PV-staircase flow [FJBV et al., 2008].
- Ocean jets; satellite altimetry data [FJBV, 2010; more in progress].

Hamiltonian setup

- Fluid particle motion develops on $\mathbb{R}^2$ obeying:

$$\dot{x} = -\partial_y \psi(x, y, t), \quad \dot{y} = +\partial_x \psi(x, y, t). \tag{1}$$

Constitutes a ***nonautonomous one-degree-of-freedom Hamiltonian system*** with ψ (streamfunction) Hamiltonian; x (zonal coordinate) coordinate; and y (meridional coordinate) momentum.

- Very good approximation for stratospheric flows (strongly stratified, predominantly balanced); harder to justify for Jovian and ocean flows.

- The streamfunction is decomposed into a steady unperturbed part (undulating zonal jet) plus an unsteady perturbation (traveling waves):

$$\psi(x, y, t) = h(x, y) + \varepsilon r(x, y, \Omega_1 t, \cdots, \Omega_N t), \tag{2}$$

Here $\Omega_n t \in \mathbb{T}(= \mathbb{R}/2\pi\mathbb{Z})$ where $\{\Omega_n\}$ are (relative) wave frequencies and x moves with the speed of one of the waves.

- In a neighborhood of the jet's axis we introduce ***action–angle variables*** $(I, \theta) \in D \times \mathbb{T}$, where $D \subset \mathbb{R}$ is closed and bounded:

$$I := \frac{1}{2\pi} \oint X(y;h)\mathrm{d}y, \; \theta := \partial_I G, \; G(y, I) := \int_0^y X(\xi;h)\mathrm{d}\xi, \quad (3)$$

where X is the (moving) zonal coordinate of an isoline of h.

- Background and perturbation Hamiltonian take the forms:

$$h(x, y) = H(I), \quad (4a)$$

$$r(x, y, \Omega_1 t, \cdots, \Omega_N t) = R(I, \theta, \Omega_1 t, \cdots, \Omega_N t). \quad (4b)$$

The variables (I, θ) evolve according to:

$$\dot{I} = -\varepsilon \partial_\theta R, \quad \dot{\theta} = \omega(I) + \varepsilon \partial_I R, \quad (4c)$$

where

$$\omega(I) := H'(I). \quad (4d)$$

KAM theorem for time-quasiperiodic Hamiltonians

Theorem. *If the Hamiltonian* $H(I) + \varepsilon R(I, \theta, \Omega_1 t, \cdots, \Omega_N t)$ *is sufficiently smooth, if* $\varepsilon > 0$ *is sufficiently small, the forcing frequencies* $\{\Omega_n\}$ *are sufficiently irrational, and unperturbed frequency* $\omega(I) = H'(I)$ *is not a constant, then the Hamiltonian* $H + \varepsilon R$ *admits a measure-theoretically large set of invariant tori close to* $\{I = \mathrm{const}\}$ *with frequency* $\varpi(I)$ *close to* $\omega(I)$ *which vibrate with frequencies* $\{\Omega_n\}$.

Proof. Uses Broer–Huitema–Takens theory of "unfoldings" of invariant tori [cf. Sevryuk 2007].

Discrete and Continuous Dynamical Systems (DCDS-A)

Pages: 569 - 595, Volume: 18 , Issue: 2/3, June , July 2007

Invariant tori in quasi-periodic non-autonomous dynamical systems via Herman's method

doi:10.3934/dcds.2007.18.569 About DOI Full text: PDF (313.8K) Cited By Purchase Paper (30.00 USD)

Mikhail B. Sevryuk - Institute of Energy Problems of Chemical Physics, The Russia Academy of Sciences, Leninskiĭ prospect 38, Bldg. 2, Moscow 119334, Russian Federation (email)

Abstract: We consider quasi-periodic (with N basic frequencies) non-autonomous perturbations of Hamiltonian, reversible, volume preserving, and dissipative systems. The unperturbed systems possess analytic families of invariant n-tori carrying conditionally periodic motions, are allowed to depend on external parameters, and are assumed to satisfy just very weak nondegeneracy conditions. We construct invariant $(n+N)$-tori in perturbed systems following M.R. Herman's approach: additional external parameters are introduced to remove degeneracies and then are eliminated via an appropriate number-theoretical lemma concerning Diophantine approximations of dependent quantities.

Keywords: KAM theory, quasi-periodic perturbations, quasi-periodic motions, invariant tori, Herman's method.
Mathematics Subject Classification: 37J40, 70H08, 70K43, 70H33.

Received: December 2005; **Revised:** May 2006; **Published:** March 2007.

Remarks

- Admitted tori are Lagrangian (i.e., of maximal dimension), and thus act as meridional transport barriers.
- Nondegeneracy condition $\omega(I) \neq$ const differs from standard (Kolmogorov) nondegeneracy condition $\omega'(I) \neq 0$:
  - ▷ very weak nondegeneracy condition of Russmann's type;
  - ▷ allows one to prove admittance of many invariant tori even when the "twist" vanishes ($\omega'(I) = 0$) at isolated I-values;
  - ▷ the relevance is that at a zonal jet's axis the frequency of particle motion has a local extremum, and hence $\omega'(I) = 0$ there.
- Unlike standard KAM theory, the frequency along admitted perturbed tori cannot be related with the frequency along unperturbed tori:
  - ▷ prevents one from speaking about "persistence" of invariant tori [Sevryuk, 1995];
  - ▷ for our purposes what really matters is that invariant tori can be proved to be present, and that they serve as transport barriers.

“Strong KAM stability”

We have seen that many tori of $H(I) + \varepsilon R(I, \theta, \Omega_1 t, \cdots, \Omega_N t)$ can be proved to “persist” a perturbation under certain conditions. We now consider the possibility that degenerate (twistless) tori are more resistant than nondegenerate ones.

A simple example of "strong KAM stability"

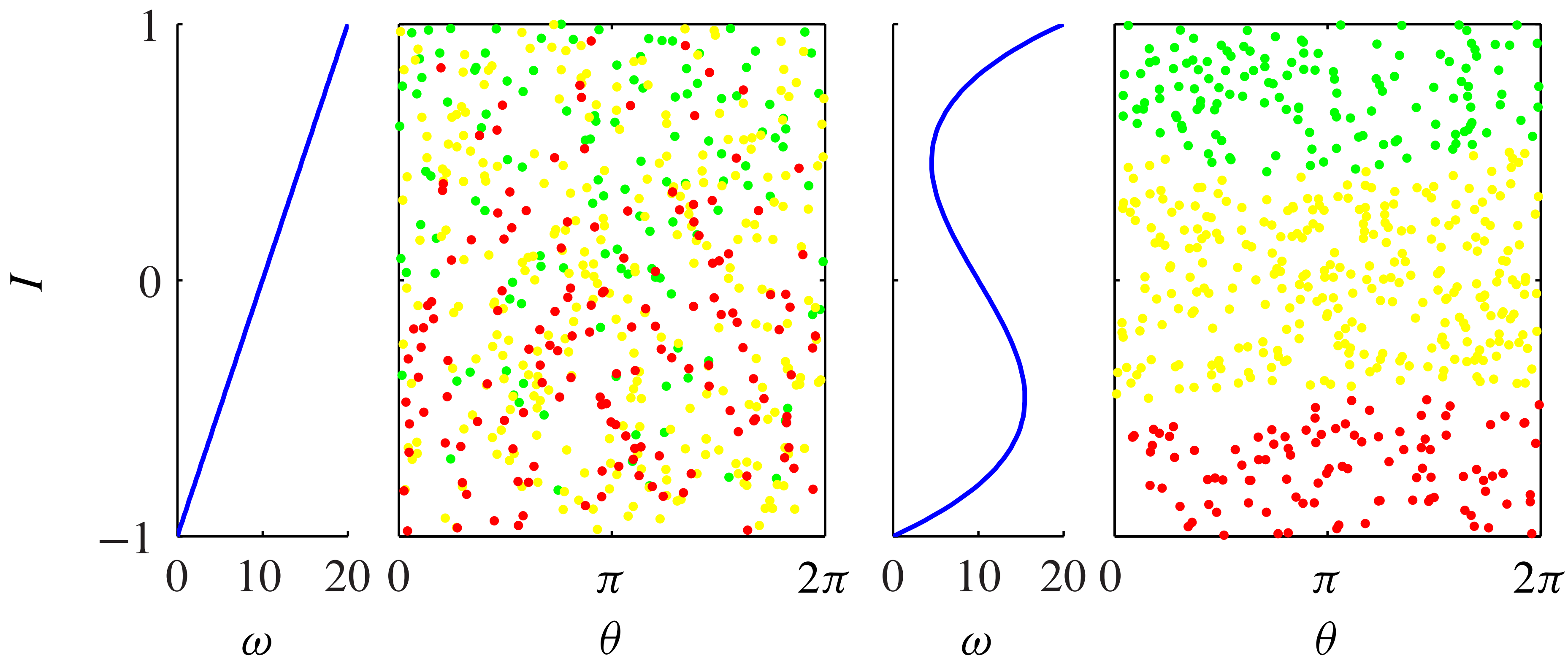

The integrable Hamiltonian $H = \int \omega(I)\,\mathrm{d}I$ and the nonintegrable Hamiltonian perturbation with

$$R = \cos(I + \theta) \sum_{n=1}^{21} \cos \Omega_n t, \quad \Omega_n = n + \nu_n,$$

where $\{\nu_n\}$ are small and random and $\varepsilon = 0.025$.

Resonance widths

- Torus destruction is accomplished via resonance (i.e., when $\omega(I)/\Omega_n \in \mathbb{Q}$ for some n).
- The ***resonance widths***:

$$\text{nondegenerate torus}: \Delta\omega \sim \varepsilon^{1/2}|\omega'(I)|^{1/2}$$

vs

$$\text{degenerate torus}: \Delta\omega \sim \varepsilon^{2/3}|\omega''(I)|^{2/3}.$$

▷ Resonance widths are smaller for degenerate tori, there is less possibility of frequency overlapping, and hence degenerate tori may be expected to be more stable than nondegenerate tori.

▷ This type of stability has been referred to as "strong KAM stability" in Rypina et al. [2007a].

KAM-like LCS identification

- Traditional phase space visualization techniques, such as the Poincaré section, are not available when the Hamiltonian is time aperiodic or given as a data set.
- The ***Finite-Time Lyapunov Exponent (FTLE)***, defined by

$$\Lambda_{t_0}^{\tau}(\boldsymbol{x}_0) := (2|\tau|)^{-1} \ln \lambda_{\max} \boldsymbol{C}_{t_0}^{t_0+\tau}(\boldsymbol{x}_0) \tag{5}$$

  where $\boldsymbol{C}_{t_0}^{t_0+\tau}(\boldsymbol{x}_0)$ is the ***Cauchy–Green deformation tensor***. Local maximizing curves or ridges of this field have been used to diagnose hyperbolic LCS [Haller 2001, 2002].
- Because trajectories lying on invariant tori are regular, their *infinite-time* LE are typically zero.
  - ▷ FJBV et al. [2010] proposed that KAM-like LCS (a type of elliptic LCS) should be identified as *topologically circular trenches of backward-plus-forward* FTLE field.
  - ▷ FJBV et al. [2010] noted that *twistless* KAM-like LCS should be most easily identified using this technique.

Twistless tori and FTLE trenches

- In the integrable case $\dot{I} = 0$, $\dot{\theta} = \omega(I)$ we have:

$$\Lambda = \frac{1}{2|\tau|} \ln \left(\frac{2 + \omega'(I)^2\tau^2}{2} + \sqrt{\frac{\left(2 + \omega'(I)^2\tau^2\right)^2}{4} - 1} \right).$$

  - ▷ As expected $\lim_{\tau\to\pm\infty} \Lambda = 0$.
  - ▷ But for finite τ, Λ increases as $\omega'(I)$ increases (and vanishes when $\omega'(I) = 0$).
  - ▷ For finite τ, the tori for which $|\omega'(I)|$ is maximized produce ridges in the FTLE field. Moreover, $\Lambda \sim |\tau|^{-1} \ln |\omega'(I)\tau|$ for fixed $\omega'(I) \neq 0$ as $\tau \to \pm\infty$, which tends to 0 slowly. This may make it difficult to identify regular trajectories.
  - ▷ But this ambiguity is reduced when $|\omega'(I)|$ is small.
- Twistless tori are thus the ones that can be most easily detected using FTLE.

The Bickley jet

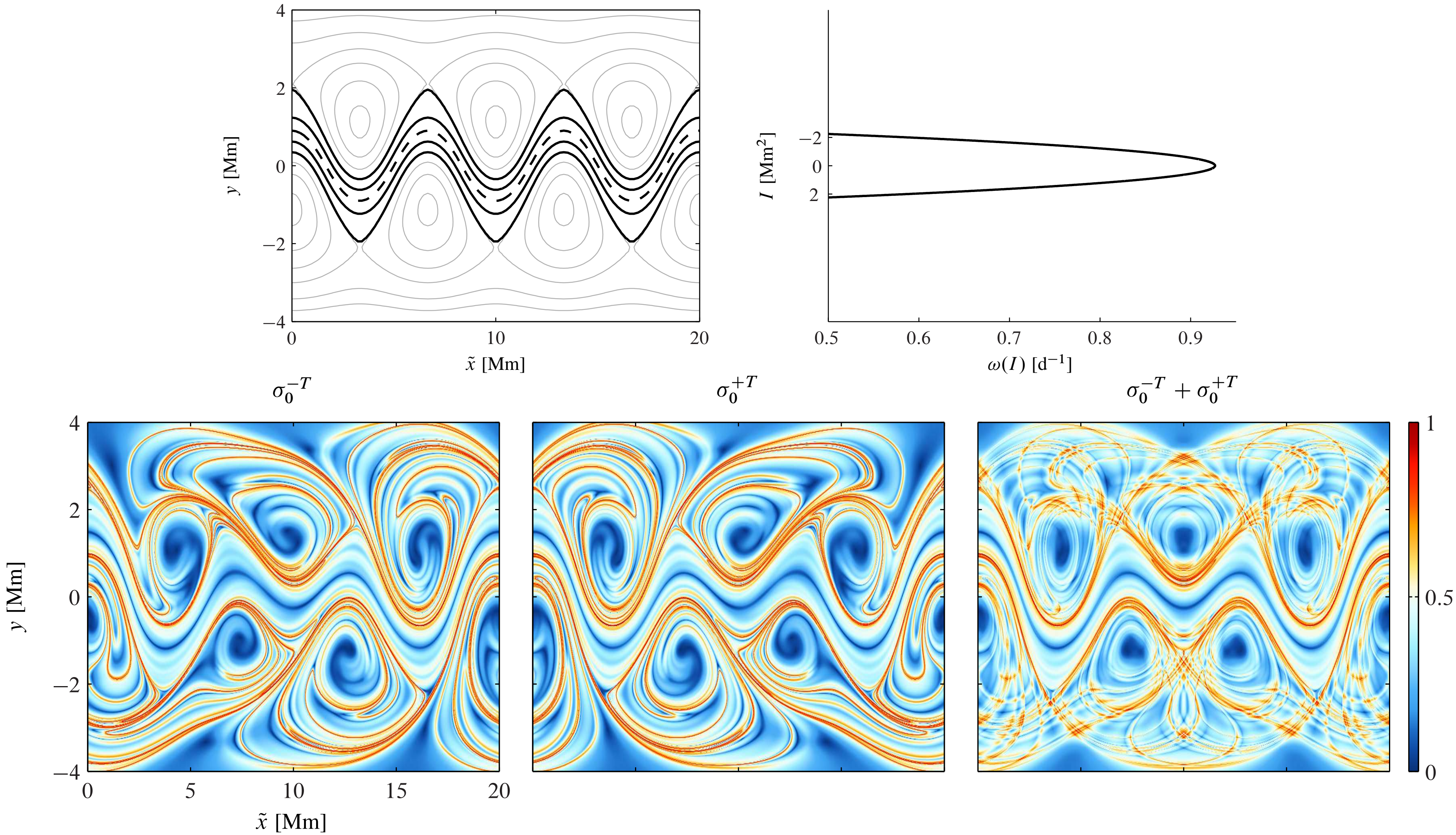

Note the thin band free of hyperbolic LCS near the jet axis; corresponds to elliptic LCS. Being KAM-like can be identified as connected trenches of backward-plus-forward FTLE field [FJBV et al., 2010].

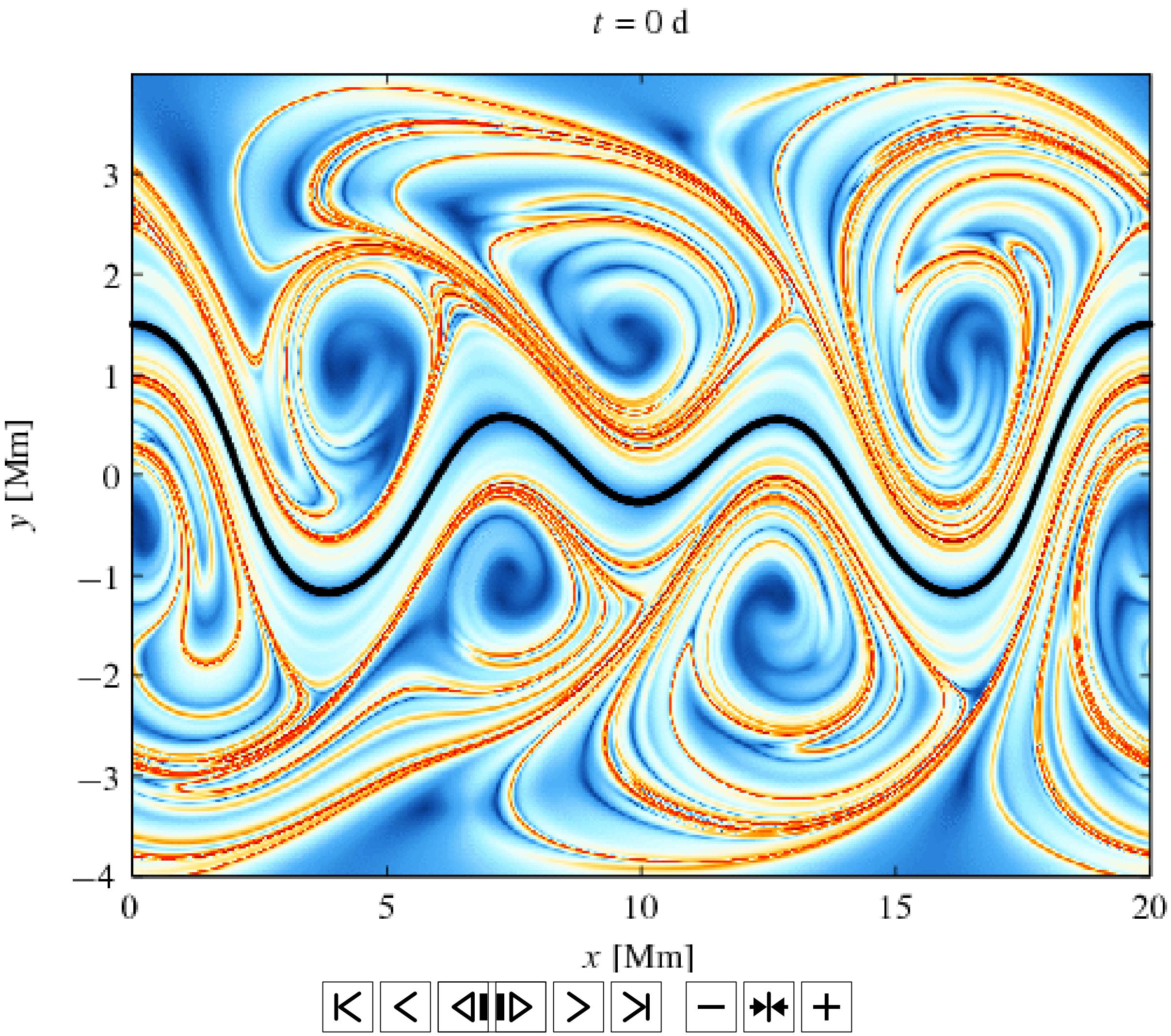

Trajectory integration confirms that identified FTLE trench is the locus of an invariant set.

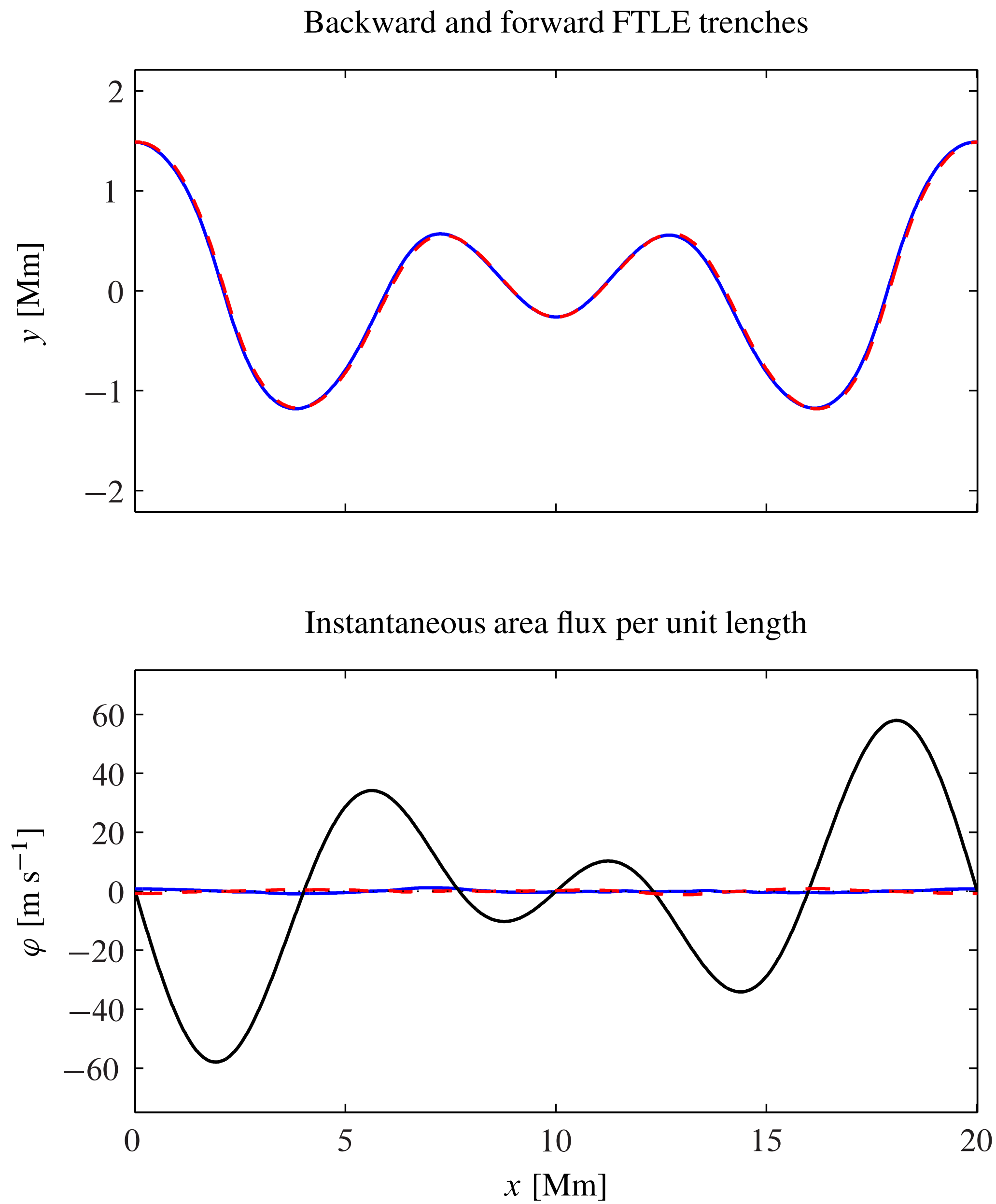

Flux estimate through FTLE trench is vanishingly small.

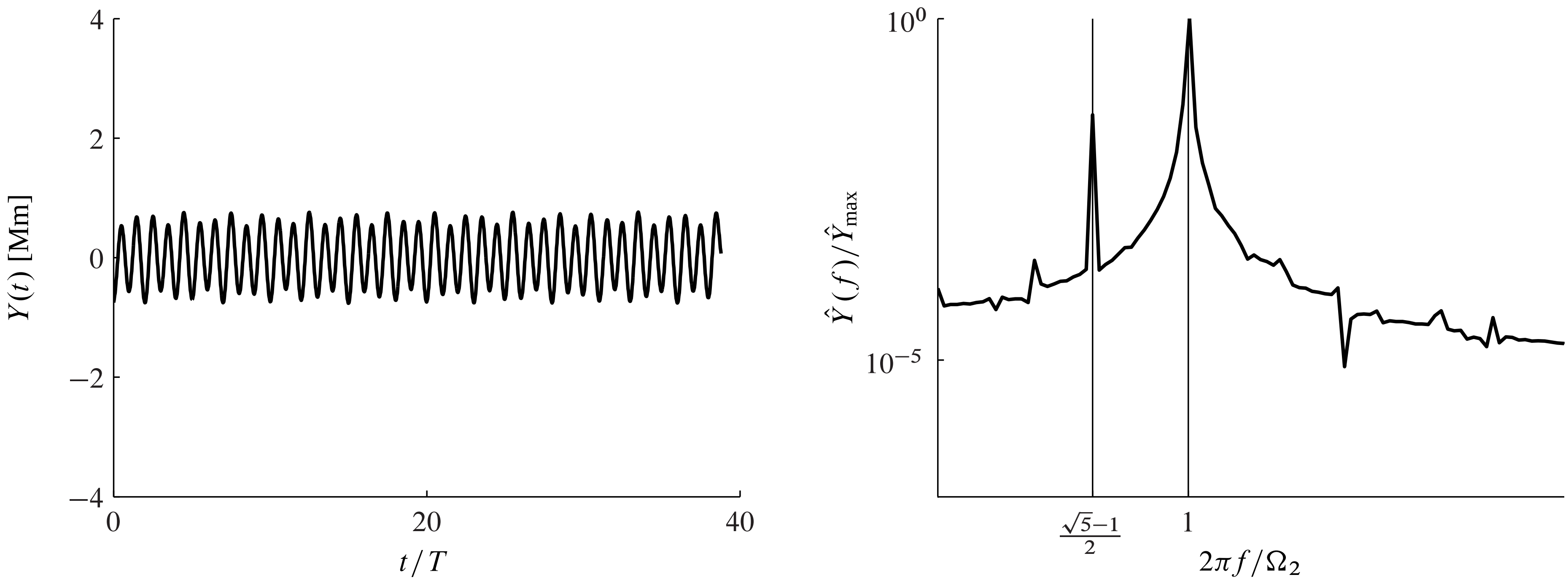

The KAM-like LCS "dances" with the two (irrationally related) frequencies of the perturbation field.

Stratospheric jets

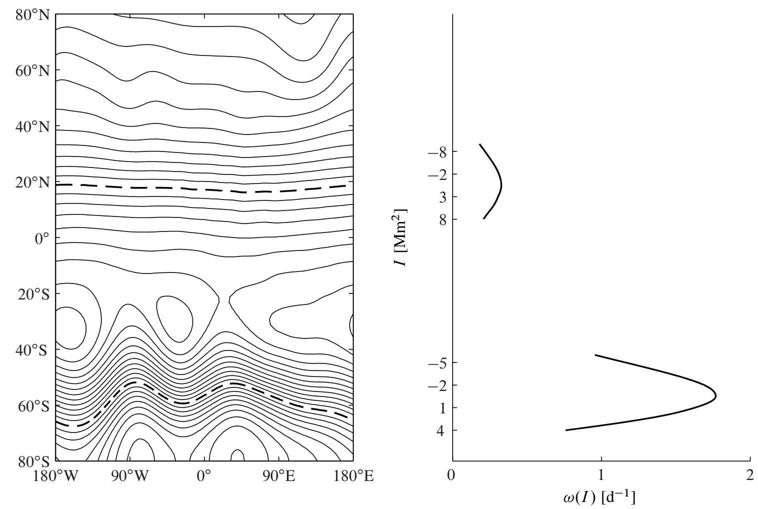

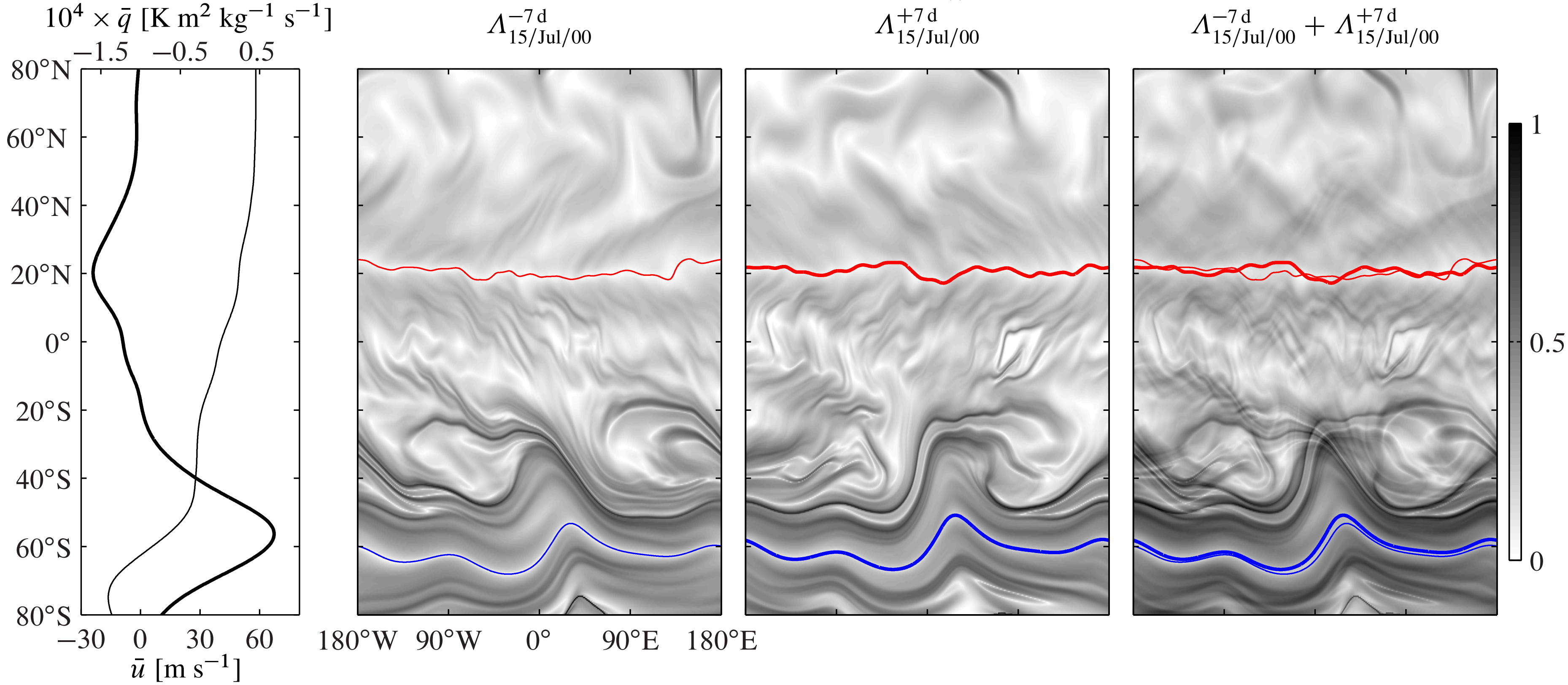

Trajectory integration on Jul—jets present near 20°N and 60°S

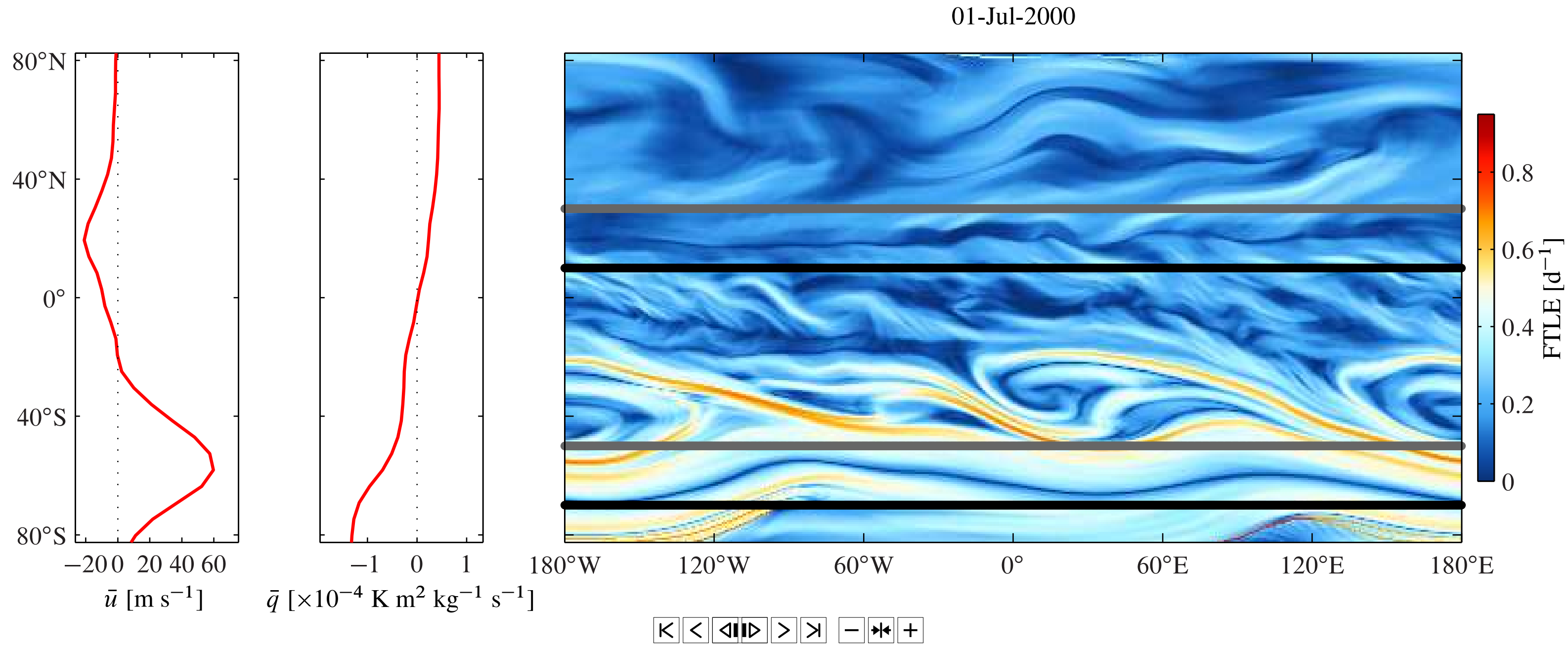

Trajectory integration on Jan—jets absent near 20°N and 60°S

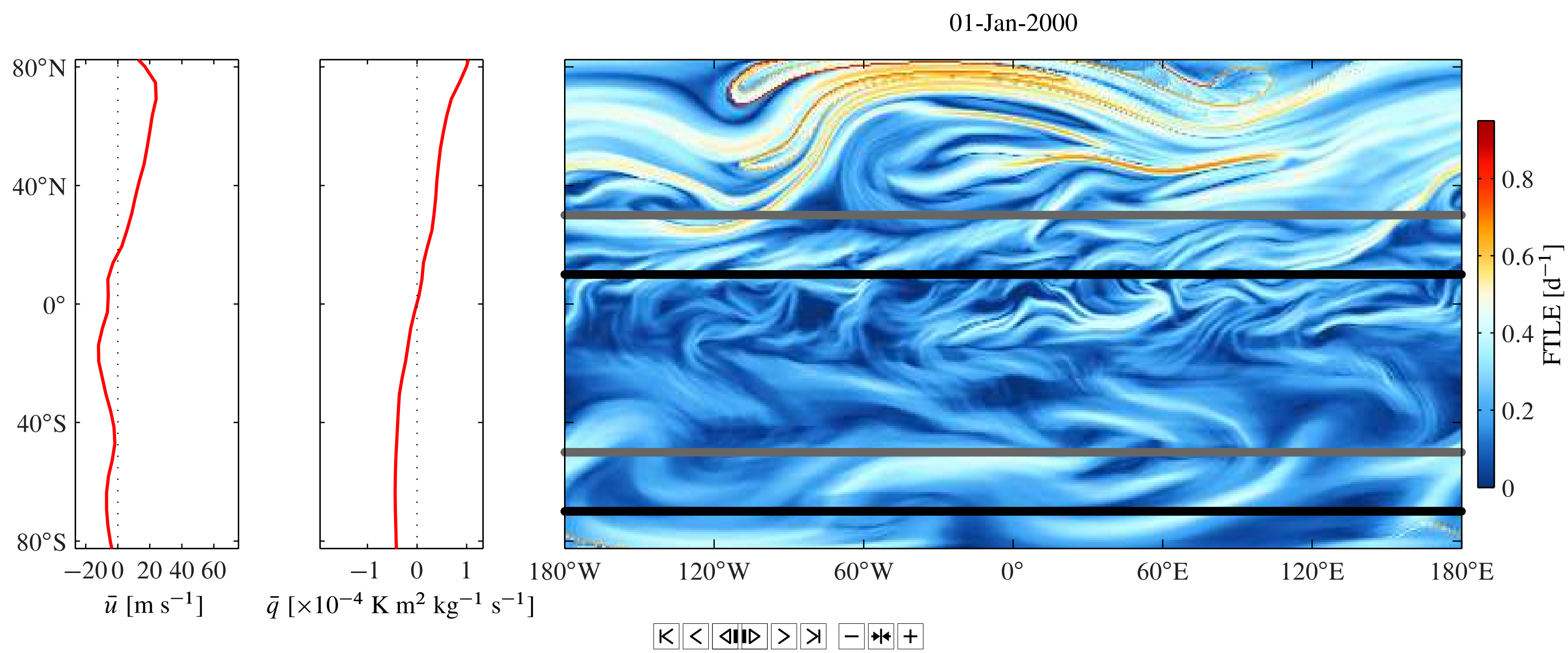

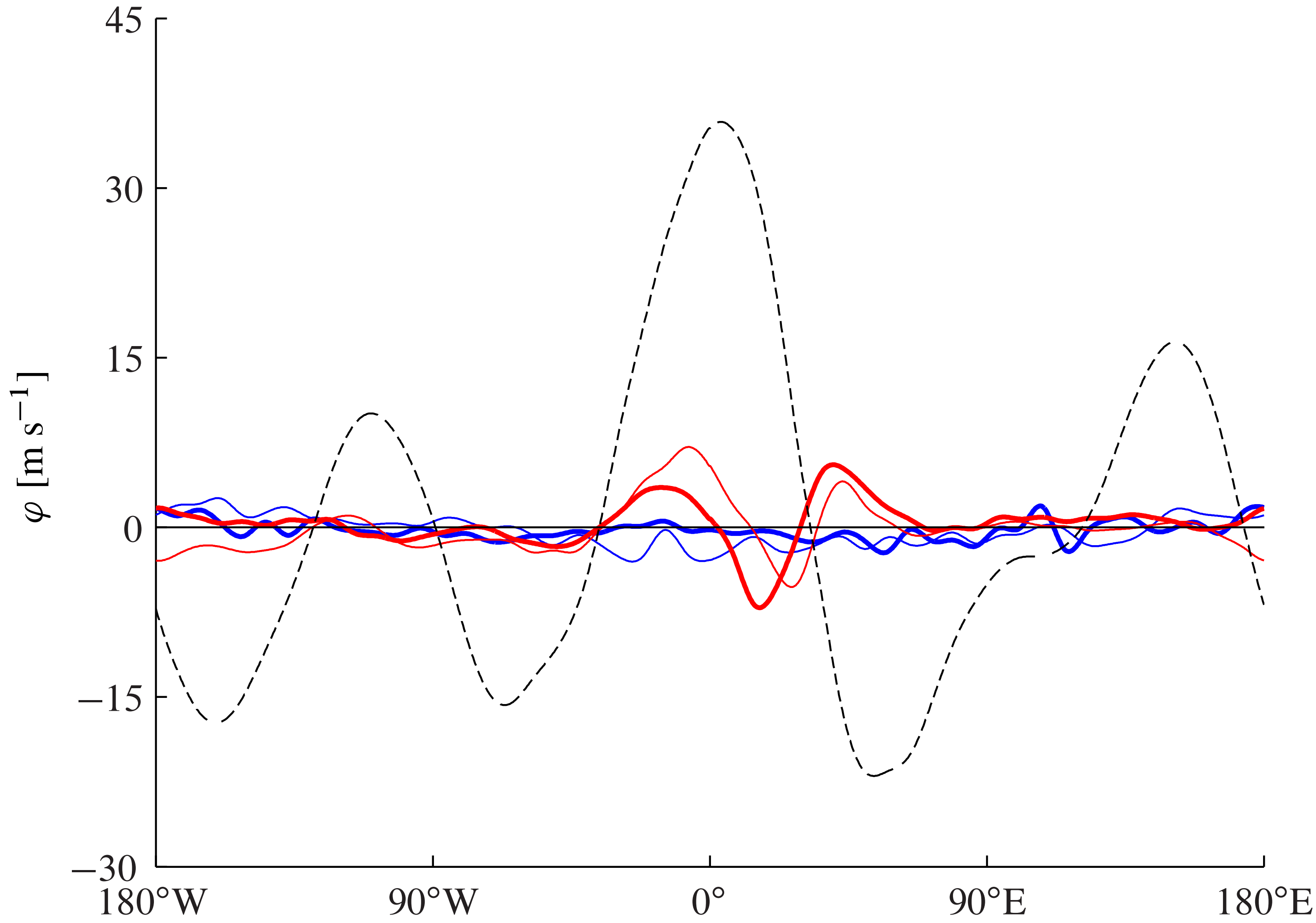

Flux estimates through FTLE trenches are fairly small.

Jovian jets

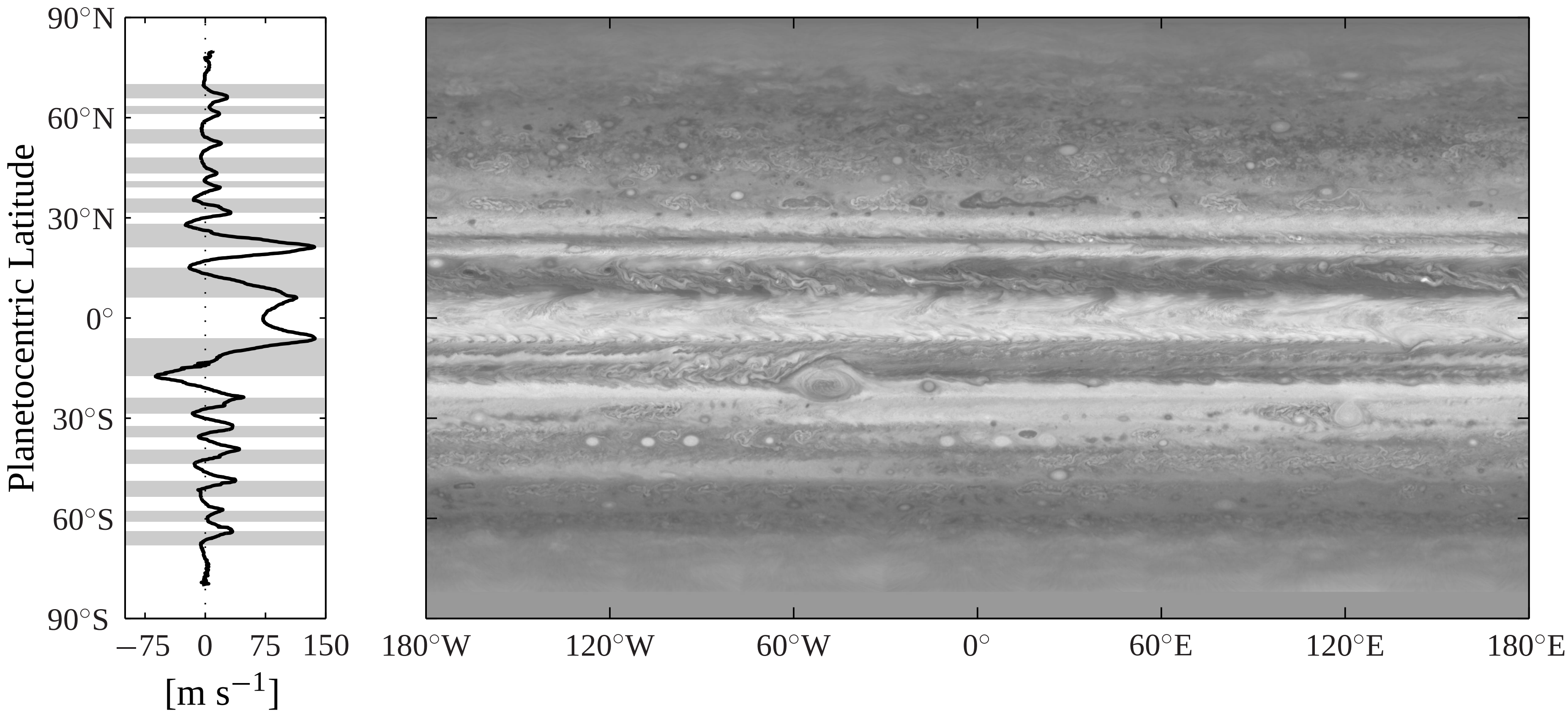

Planetocentric Latitude
90°N
60°N
30°N
0°
30°S
60°S
90°S
−75
0
75
150
[m s^{-1}]
180°W
120°W
60°W
0°
60°E
120°E
180°E

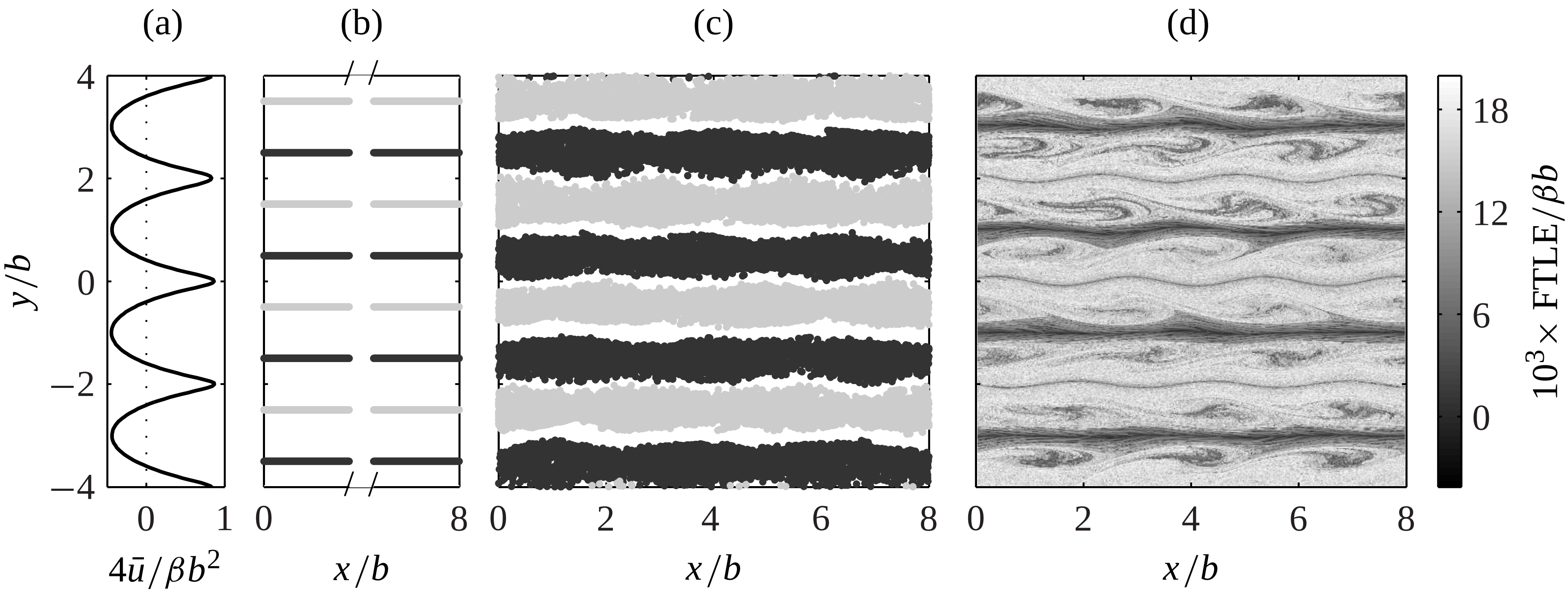

Trajectory integration and FTLE calculation based on velocity field consistent with a nonlinear simulation based on the quasigeostrophic PV equation initialized from a perturbed PV-staircase flow (i.e., with step-like PV and alternating eastward and westward jets.

Southern Ocean jets

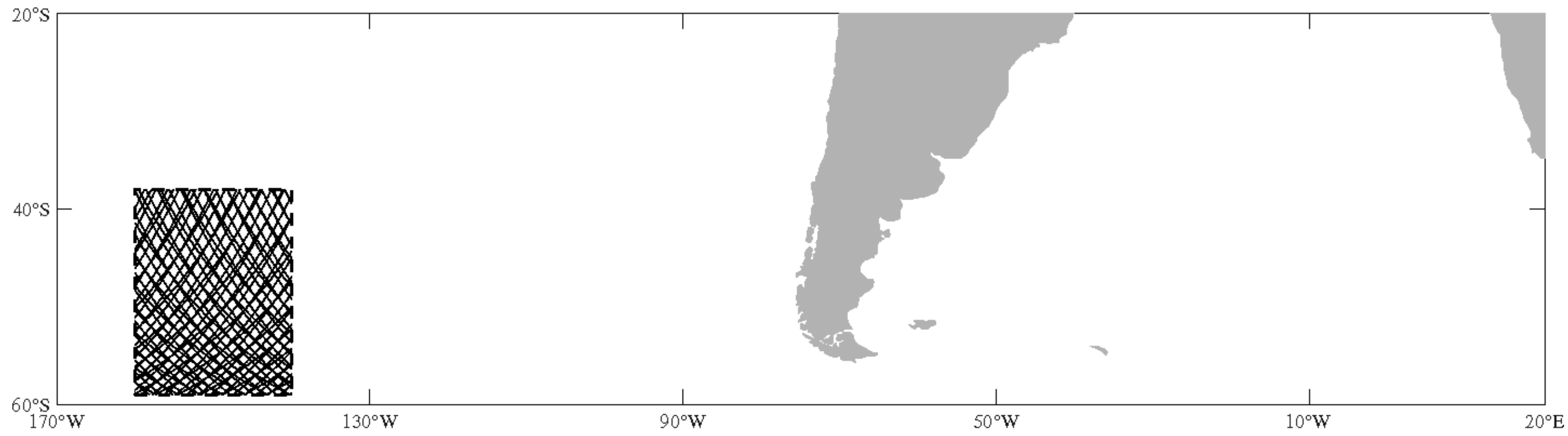

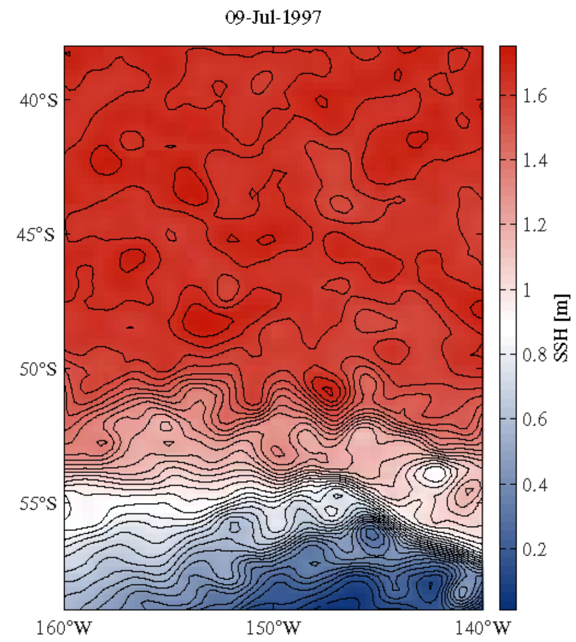

Satellite altimetric sea surface topography (streamfunction) reveals jets in the Pacific Sector of Southern Ocean.

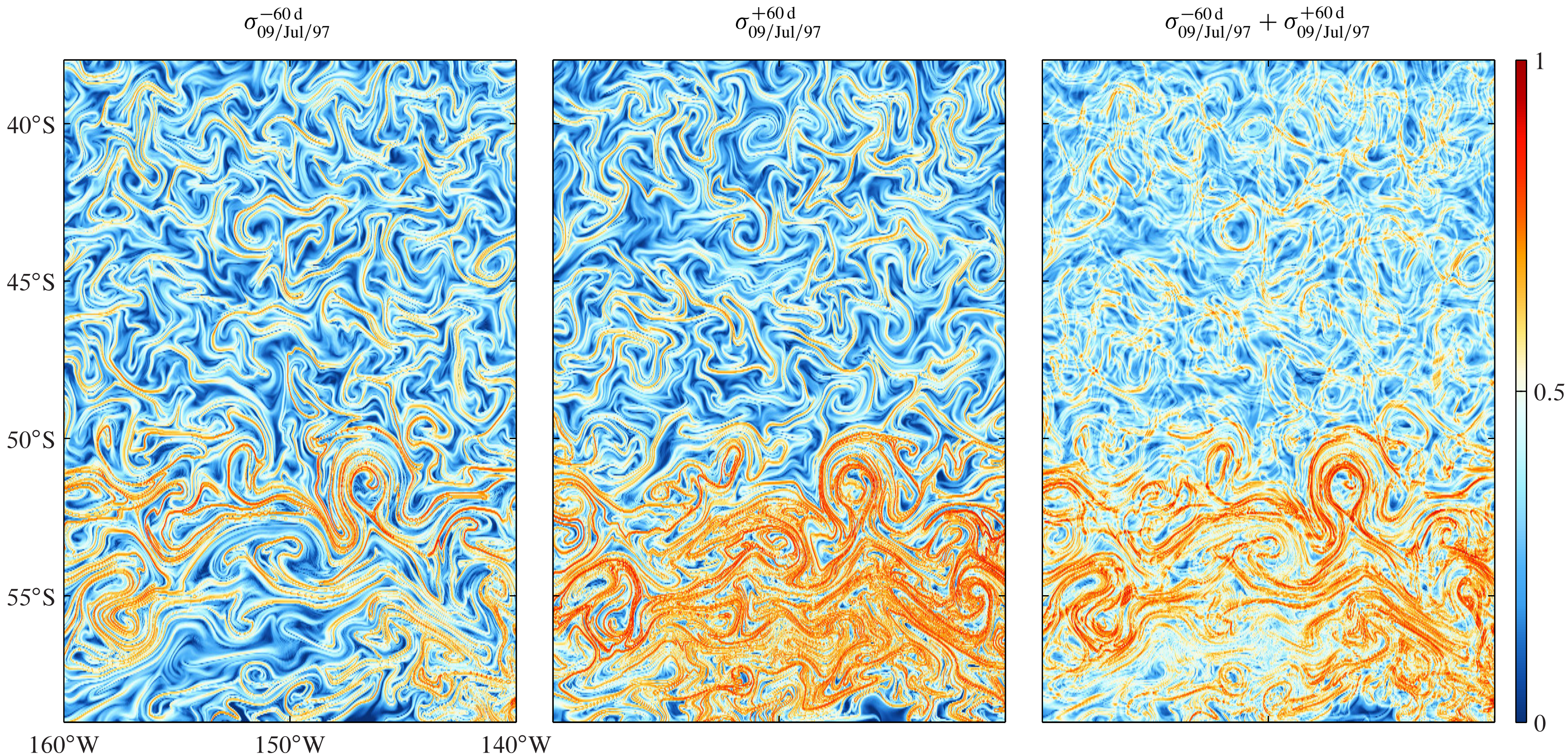

FTLE calculation insinuates the presence of features with properties similar to KAM-like LCS.

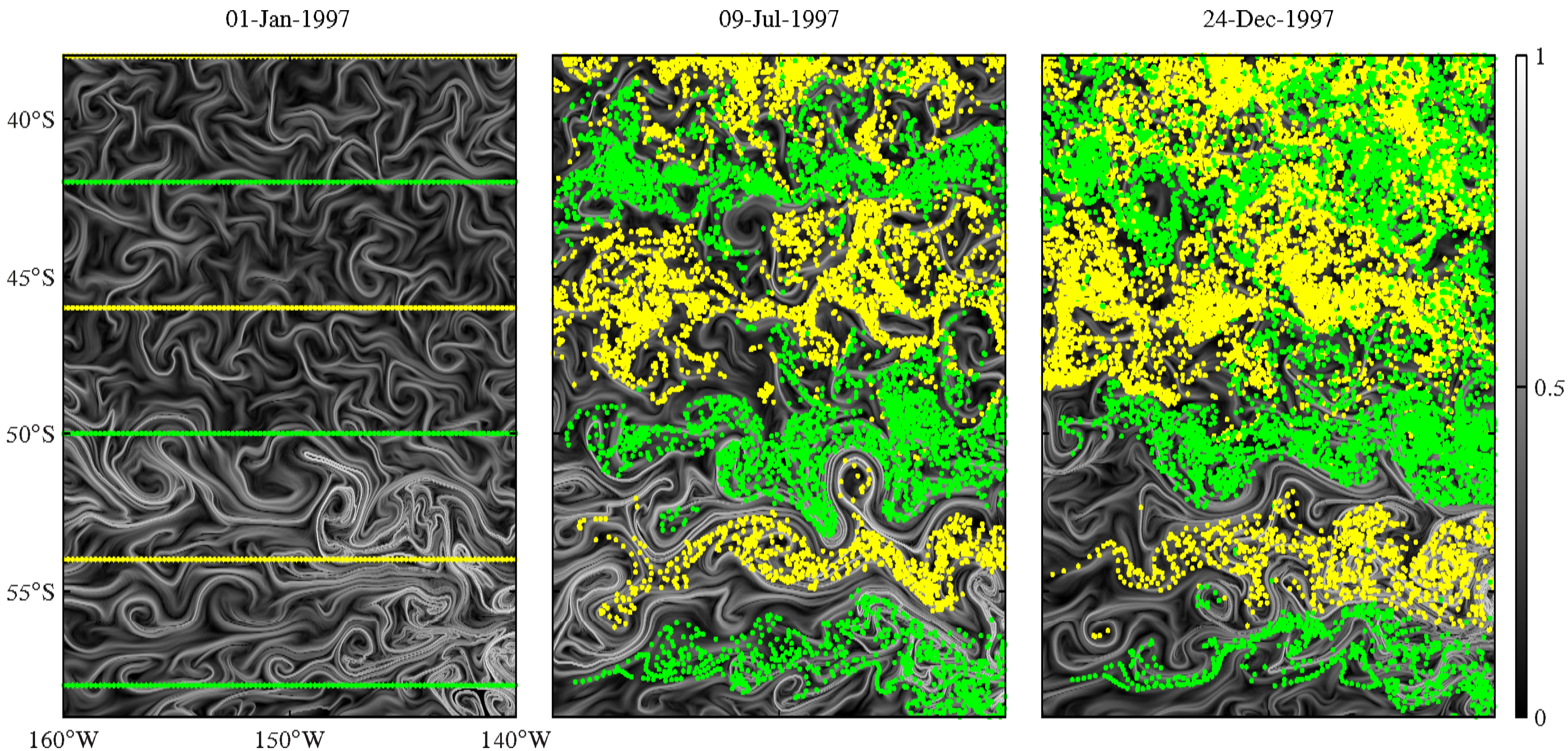

Trajectory integration reveals the presence of meridional transport barriers.

Summary

- This talked has dealt with Lagrangian Coherent Structures (LCS) of elliptic class—material curves that do not exhibit exponential stretching and folding over a finite-time interval.
- Unlike hyperbolic LCS, which facilitate mixing, elliptic LCS prevent mixing; both comprise the “skeleton” of the Lagrangian circulation.
- Recent KAM-theory-related work has associated of elliptic LCS analogous to KAM tori with zonal jet streams.
- Using a kinematic model of a perturbed meandering zonal jet, we have shown that KAM-like LCS can be identified as connected trenches of backward-plus-forward FTLE field.
- We have illustrated the presence of KAM-like LCS in stratospheric winds produced by a realistic GCM.
- We have demonstrated the occurrence of KAM-like LCS in the presence of Jovian-like jets and shown that KAM-like LCS may be also found in the ocean.

Topics of future research

- Seasonality of stratospheric flows requires KAM theory to be extended to topology changing unperturbed Hamiltonians.
- Nonzonal oceanic jets can sustain KAM-like LCS (e.g., Gulf Stream). However, lack of periodicity calls for a different identification technique and appropriate physical/mathematical definition of elliptic LCS.

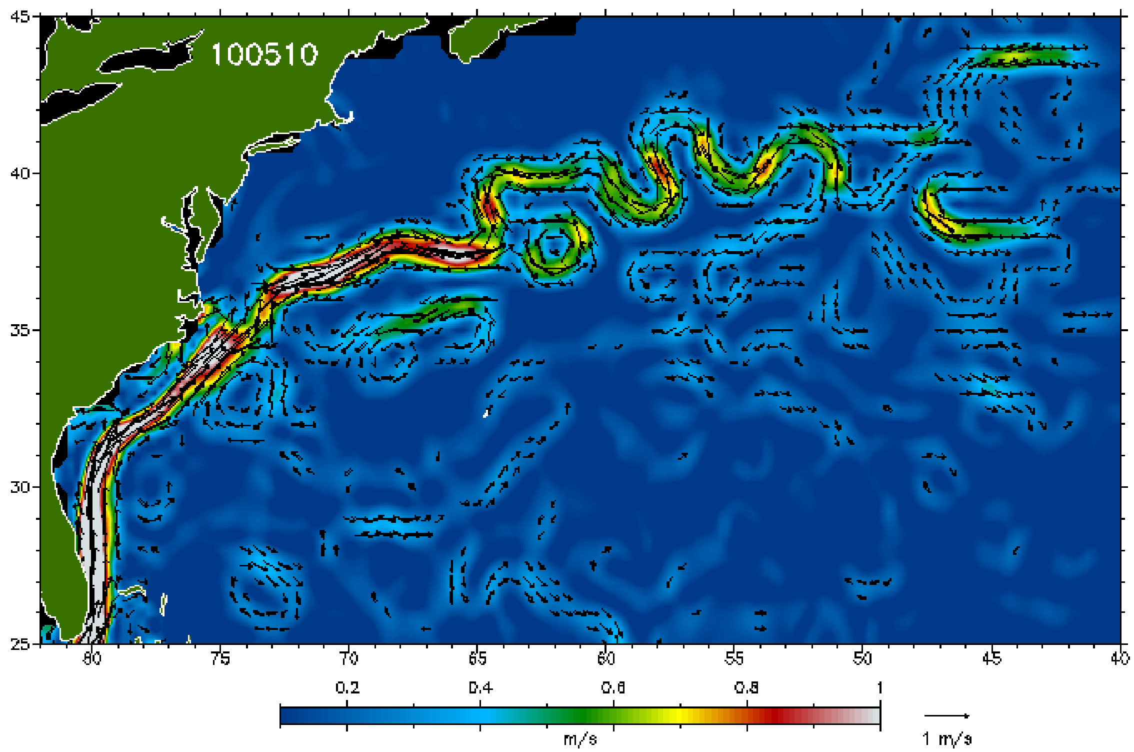

References

FJBV [2010]. *J. Geophys. Res.* 15, C10027.

FJBV et al. [2011]. *J. Atmos. Sci.*, submitted.

FJBV et al. [2010]. *Chaos* 20, 017514.

FJBV et al. [2008]. *J. Atmos. Sci.* 65, 3316.

del-Castillo-Negrete and Morrison [1993]. *Phys. Fluids A* 5, 948.

Haller [2011]. *Physica D* 240, 574.

Haller [2002]. *Phys. Fluids* 14, 1851.

Haller [2001]. *Phys. Fluids* 13, 3365.

Haller and Yuan (2000). *Physica D* 147, 352.

Rypina et al. [2007a]. *Phys. Rev. Lett.* 98, 104102.

Rypina et al. [2007b]. *J. Atmos. Sci.* 64, 3595.

Sevryuk [2007]. *Dis. Cont. Dyn. Sys. A* 18, 569.

Sevryuk [1995]. *J. Dyn. Cont. Sys.* 1, 351.

Dank u wel.